The Journal of Neuroscience, February 1, 2000, 20(3):1260–1271

A Developmental Change in NMDA Receptor-Associated Proteins at Hippocampal Synapses

Nathalie Sans,[1] Ronald S. Petralia,[1] Ya-Xian Wang,[1] Jaroslav Blahos II,[1] Johannes W. Hell,[2] and Robert J. Wenthold[1]

[1]*Laboratory of Neurochemistry, National Institute on Deafness and Other Communication Disorders, National Institutes of Health, Bethesda, Maryland 20892, and* [2]*Department of Pharmacology, University of Wisconsin, Madison, Wisconsin 53706-1532*

The membrane-associated guanylate kinases [Chapsyn-110/postsynaptic density-93 (PSD-93), synapse-associated protein-90 (SAP-90)/PSD-95, and SAP-102] are believed to cluster and anchor NMDA receptors at the synapse and to play a role in signal transduction. We have investigated the developmental changes in expression of these proteins in rat hippocampus using biochemical analyses and quantitative immunogold electron microscopy. At postnatal day 2 (P2), SAP-102 was highly expressed, whereas PSD-93 and PSD-95 were low. SAP-102 expression increased during the first week, stayed stable through P35, and showed a reduced expression at 6 months. From P2 through 6 months, PSD-93 and PSD-95 increased. For PSD-95, the percent of labeled synapses increased almost threefold with age, whereas the number of gold particles per labeled synapse did not change significantly, suggesting that the increase in PSD-95 is attributable primarily to an increase in the number of synapses containing PSD-95. In contrast, for SAP-102, both percent labeled synapses and the number of gold particles per labeled synapse decreased during this time. From Western blots of hippocampus and immunogold analysis of CA1 synapses, the high expression of NR2B at P2 coincides with the high level of SAP-102 at synapses, whereas the later expression of NR2A coincides with that of PSD-93 and PSD-95. To determine whether the changes in PSD-93/95 and SAP-102 reflect preferred associations with NR2A and NR2B, respectively, we measured co-immunoprecipitation in the adult hippocampus. These studies suggest that there is a preference for complexes of NR2A/PSD-93/95 and NR2B/SAP-102. These results indicate that individual receptor-associated proteins may have specific functions that are critical to synapse development.

Key words: MAGUKs; PSD-93; PSD-95; SAP-102; glutamate receptors; postsynaptic density; hippocampus

The postsynaptic density (PSD), a highly organized cytoskeletal structure found adjacent to the postsynaptic membrane of excitatory synapses, is believed to play a role in the organization of receptors and related proteins involved in synaptic signaling. A number of proteins enriched in the PSD have been characterized (for review, see Kennedy, 1993, 1997); one of these, synapse-associated protein-90 (SAP-90)/postsynaptic density-95 (PSD-95), was initially identified based on its abundance in the isolated PSD (Cho et al., 1992; Kistner et al., 1993). Later studies showed that PSD-95 interacts with the C terminus of NMDA receptor NR2 subunits, suggesting that PSD-95 may play a role in the synaptic anchoring and organization of NMDA receptors (Kornau et al., 1995; Niethammer et al., 1996). Three additional proteins, structurally related to PSD-95, have been identified: SAP-97/hdlg (Lue et al., 1994; Müller et al., 1995), Chapsyn-110/PSD-93 (Brenman et al., 1996b; Kim et al., 1996), and SAP-102 (Lau et al., 1996; Müller et al., 1996) (for review, see Sheng, 1996; Sheng and Kim, 1996; Kornau et al., 1997). These proteins have three PDZ (for PSD-95, Dlg, ZO-1/Dlg-homologous region) domains, one Src homology 3 domain, and one guanylate kinase-like domain and are generically referred to as membrane-associated guanylate kinases (MAGUKs). In addition to interacting with NMDA receptors, MAGUKs interact with a series of other proteins that have structural, and perhaps signaling, functions at the synapse (for review, see Nagano et al., 1998; Kim and Huganir, 1999).

The patterns of expression of SAP-97, PSD-93, PSD-95, and SAP-102 are distinct but overlapping in brain. Although not rigorously studied, many neurons appear to express multiple MAGUKs, raising questions about their structural and functional relationships. In transfected cells, PSD-93 and PSD-95 induce the clustering of NMDA receptors and can form heteromeric complexes (Kim et al., 1995, 1996), indicating that if multiple MAGUKs are present at the same PSD, they may be structurally coupled. The possibility that individual MAGUKs can substitute for one another is suggested by the results of a study showing that mice carrying a truncated form of PSD-95 exhibited changes in NMDA receptor-related plasticity yet retained most aspects of normal NMDA receptor function (Migaud et al., 1998).

NMDA and AMPA receptors show distinct patterns of postnatal development at CA1 synapses in the hippocampus. NMDA receptors are present at synapses in the postnatal day 2 (P2) animal, indicating that the NMDA receptor anchoring and organizational machinery is already mature at P2 (Petralia et al.,

Received Aug. 3, 1999; revised Nov. 15, 1999; accepted Nov. 15, 1999.

This work was supported by the National Institute on Deafness and Other Communication Disorders intramural program (R.J.W.) and by National Institutes of Health Grant NS 35563 (J.W.H.). We thank Dr. J. Fex and members of the laboratory of R.J.W. for critical reading of this manuscript.

N.S. and R.S.P. contributed equally to this paper.

Correspondence should be addressed to Dr. Nathalie Sans, National Institute on Deafness and Other Communication Disorders, National Institutes of Health, Building 36, Room 5D08, Bethesda, MD, 20892. E-mail: sansn@nidcd.nih.gov.

Table 1. Summary of antibodies against MAGUKs used

Antibody	Name/source	Ref.[a]	Host[b]	Amino acid residues	Western blot	IP	Immunocytochemistry
SAP-97	JH62426		R	1 – 105	1/1000 (serum)	+	
PSD-93	GP-DB/Dr. D. B. Bredt	1	GP	77 – 453	1/3000 (serum)		1/100
	Gt-DB/Dr. D. B. Bredt		Gt	299 – 417	1/3000 (serum)		
	AL/Alomone Laboratories		R	336 – 379	1.7 μg/ml	+	5–20 μg/ml
	R-DB/Dr. D. B. Bredt		R	299 – 417	1/1000 (serum)		
SAP-102	JH 62514		R	1-119	1/1000 (serum)	+	3.5–10.5 μg/ml (purified)
	GP-DB/Dr. D. B. Bredt		GP	1 – 118	1/1000 (serum)		1/10 (purified)
PSD-95	Clone 6G6-1C9/Affinity BioReagents	2	M		1/2000		
	Clone 7E3-1B8/Affinity BioReagents	2	M		1/2000	+	
	TL/Transduction Laboratories		M	353 – 504	1.0 μg/ml		5 μg/ml
	T60		R	228–299	1/2000 (serum)	+	
	JH62092		R	494 – 510	0.5 μg/ml	+	7 μg/ml

[a] 1, Brenman et al. (1996a,b); 2, Kornau et al. (1995).

[b] GP, Anti-guinea pig; Gt, anti-goat; M, anti-mouse; R, anti-rabbit.

1999). However, studies on the gross developmental properties of MAGUKs show marked differences among the different members (Cho et al., 1992; Müller et al., 1996; Song et al., 1999; Wyszynski et al., 1999). This suggests that individual MAGUKs may have specific functions that are critical for synapse development.

In the present study, we investigated the expression of MAGUKs in the hippocampus of adult and developing rats. Our results show a dramatic difference in the development of synaptic PSD-93 and PSD-95 compared with that of SAP-102, indicating that a switch in the NMDA receptor anchors plays a major role in changes in synaptic plasticity in the developing animal.

MATERIALS AND METHODS

Antibody production and purification. Antibodies against MAGUKs used are listed in Table 1. To raise antibodies against SAP-90/PSD-95 (JH62092), the peptide VERREWSRLKAKDWGSS corresponding to residues 494–510 of SAP-90 (Kistner et al., 1993) was synthesized by the solid-phase method, coupled to BSA using glutaraldehyde, and dialyzed against PBS, pH 7.4 (Hell et al., 1993). The T60 anti-PSD-95 rabbit polyclonal antibody was generated against a 6xHis fusion protein corresponding to residues 228–299 of the PSD-95 sequence (Cho et al., 1992). cDNA fragments encoding the first 105 amino acid residues of SAP-97 and the first 119 amino acid residues of SAP-102 were amplified by PCR and subcloned in pGEX-2T (Pharmacia, Piscataway, NJ). The glutathione *S*-transferase (GST)-SAP-97 and GST-SAP-102 fusion proteins were expressed in *Escherichia coli* (BL21; Novagen, Madison, WI) and purified following a protocol described in Leonard et al. (1998). For affinity purification, antisera against SAP-90/PSD-95 (JH62092), SAP-97 (JH62426), or SAP-102 (JH62514) were incubated for 2–4 hr with the SAP-90-derived peptide coupled to cyanogen bromide-activated Sepharose (Amersham Pharmacia Biotech, Piscataway, NJ) (Hell et al., 1993) or GST-SAP-97(1–105) or GST-SAP-102(1–119) cross-linked with dimethyl pimelimidate to glutathione-Sepharose (Bar-Peled and Raikhel, 1996), respectively. Antibodies were eluted with 5 ml of 3 M $MgCl_2$, and the eluate was diluted immediately with 10 ml of Tris-buffered saline (TBS) and concentrated using a Centriprep 30 concentrator from Amicon (Beverly, MA) (Hell et al., 1993).

Three anti-PSD-93 antibodies and the guinea pig anti-SAP-102 antibody were kindly provided by Dr. D. S. Bredt (University of California, San Francisco, CA) (Table 1).

The glutamate receptor antibodies were characterized previously. Rabbit polyclonal antibodies were anti-GluR1 and anti-GluR2/3 (Wenthold et al., 1992), T46 anti-NR1 (Petralia et al., 1994a), T58 anti-NR2A and T51 anti-NR2B (Christie et al., 1999), T12 anti-NR2A/B (Petralia et al., 1994b). Mouse monoclonal antibodies were anti-NR1 (clone 54.1; PharMingen, San Diego, CA), anti-NR2A (2F6.3D5; Hartveit et al., 1994; a gift from Dr. I. Bartke, Boehringer Mannheim, Mannheim, Germany), anti-NR2B (Transduction Laboratories, Lexington, KY). Affinity-purified horseradish peroxidase-conjugated donkey anti-rabbit and sheep anti-mouse secondary antibodies were purchased from Amersham Pharmacia Biotech. Affinity-purified horseradish peroxidase-conjugated swine anti-goat and rabbit anti-guinea pig antibodies were purchased from Boehringer Mannheim (Indianapolis, IN).

Transfection of HEK293 cells. cDNAs in eukaryotic expression vectors were kindly provided by the following: SAP-97 (Dr. Morgan Sheng), PSD-93 and PSD-95 (Dr. David S. Bredt), and SAP-102 (Dr. Richard L. Huganir). HEK293 cells were transfected using a standard calcium phosphate precipitation method using the CalPhos Mammalian Transfection Kit (Clontech, Palo Alto, CA). Transfected cells were incubated for 36 hr, washed, and harvested in PBS containing 0.5 mM EDTA. After centrifugation, cells were resuspended in 50 mM Tris-HCl, pH 7.5, containing a mixture of protease inhibitors (1 mM EDTA, 1 mM AEBSF, 50 μg/ml leupeptin, 10 μg/ml pepstatin, and 10 μg/ml aprotinin) and sonicated. Cell membranes were solubilized in SDS sample buffer and boiled for 10 min.

Preparation of tissue extracts. Hippocampi were dissected from P2, P10, P35, and 6-month-old Sprague Dawley rats and placed in ice-cold PBS, pH 7.4. Frozen hippocampi were homogenized in PBS, and then an equal volume of 2× SDS sample buffer was added, and the samples were boiled. Protein concentrations were measured using a BCA kit (Pierce, Rockford, IL) or a protein assay kit (Bio-Rad, Hercules, CA). Twenty micrograms of proteins were loaded in each lane for a subsequent Western blot analysis.

Immunoprecipitation. Immunoprecipitation experiments were performed as described previously (Blahos and Wenthold, 1996). Whole hippocampus or the CA1 region of P35 Sprague Dawley rats was homogenized with a Polytron in 50 mM Tris-HCl, pH 7.4, containing the protease inhibitor mixture described above. Membranes were sedimented by centrifugation (100,000 × *g*, 30 min, 4°C) and solubilized in 1% deoxycholate (DOC), 50 mM Tris-HCl, and 1 mM EDTA, pH 9, for 45 min at 37°C. Insoluble material was removed by centrifugation. Triton X-100 was added to a final concentration of 0.1%, and the supernatant was dialyzed for 16 hr against 50 mM Tris, pH 7.5, containing 0.1% Triton X-100. Insoluble material was removed by centrifugation, and the supernatant was stored at −80°C until the immunoprecipitation reactions were performed. For immunoprecipitation, 10 μl of the appropriate antiserum was added to 50 μl (resuspended resin) of protein A- or protein G-agarose beads (Pierce, Rockford, IL) in PBS containing 0.1% Triton X-100 for at least 2 hr at 4°C. Protein A or protein G beads were then pelleted, washed in PBS plus 0.1% Triton X-100, and incubated with 1 ml of the detergent-solubilized fraction at 4°C with constant rotation. The beads were then washed with 50 mM Tris-HCl, pH 7.5, containing 0.1% Triton X-100 and 150 mM NaCl. After the last wash, the beads were resuspended in 2× SDS sample buffer (100 μl) and boiled for 3 min. After the chemiluminescence detection, films were scanned using a Molecular Dynamics (Sunnyvale, CA) densitometer to estimate the amount of immunoreactivity in the bound fractions compared with that in the corresponding input fraction. Different amounts of the input were run and compared with the bound fraction.

SDS-PAGE and immunoblot analysis. Proteins were separated with

SDS-PAGE (4–20% gradient gels) and transferred to an Immobilon-P membrane (Millipore, Bedford, MA). Membranes were incubated with 5% (w/v) skim milk in TBS containing 0.05% Tween 20 overnight at 4°C. Membranes were washed and incubated with primary antibody at concentrations noted in Table 1 or using the following concentrations: GluR1, 0.5 μg/ml; GluR2/3, 0.15 μg/ml; T46 NR1, 0.5 μg/ml; clone 54.1 NR1, 1:5000; T58 NR2A, 1:2000; NR2A (2F6.3D5), 1:5000; T51 NR2B, 1:4000; NR2B monoclonal, 2.0 μg/ml; and T12 NR2A/B, 0.5 μg/ml. Immunoreactive bands were visualized with chemiluminescence (Pierce). To reprobe, blots were stripped by shaking in 2% (w/v) SDS, 62.5 mM Tris-HCl, pH 6.8, and 100 mM β-mercaptoethanol for 30 min at 60°C. Each experiment was repeated several times, and representative blots are shown. For quantification, films were scanned, and densitometry was done using a Molecular Dynamics densitometer.

Postembedding immunogold immunocytochemistry. The postembedding method has been described (Petralia et al., 1997, 1998, 1999; Rubio and Wenthold, 1997; Wang et al., 1998; Zhao et al., 1998) and is modified from a previous study (Matsubara et al., 1996). Sprague Dawley rats were anesthetized and perfused with 4% paraformaldehyde plus 0.5% glutaraldehyde in 0.1 M phosphate buffer. Two animals were used for P2, P10, and P35 and one animal for 6 months for the main studies of PSD-95 (TL) and SAP-102 (JH62514). One animal per age (P2, P10, and P35) was used for additional antibodies [PSD-95 (JH62092), SAP-102 (GP-DB), PSD-93 (GP-DB), and PSD-93 (AL)]. Parasagittal sections of the hippocampus were cryoprotected in 30% glycerol and frozen in liquid propane in a Leica (Vienna, Austria) EM CPC (Universal Cryoworkstation). Frozen sections were immersed in 1.5% uranyl acetate in methanol at −90°C in a Leica AFS freeze-substitution instrument, infiltrated with Lowicryl HM-20 resin at −45°C, and polymerized with ultraviolet light. Thin sections of the hippocampus were incubated in 0.1% sodium borohydride plus 50 mM glycine in TBS and 0.1% Triton X-100 (TBST), followed by 10% normal goat serum (NGS) in TBST, primary antibody in 1% NGS in TBST, and immunogold (10 nm; Amersham Pharmacia Biotech) in 1% NGS in TBST plus 0.5% polyethylene glycol, and the sections were stained finally in uranyl acetate and lead citrate. For double labeling using antibodies made in different species, sections were incubated with two primary antibodies [PSD-95 (TL) monoclonal plus either SAP-102 (JH62514) or GluR2/3 polyclonal (2 μg/ml)] and later incubated with two immunogolds (15 nm goat anti-mouse and 5 nm goat anti-rabbit). Other combinations included PSD-95 (TL) plus NR2A/B (T12; 4 μg/ml) or PSD-93 (AL), using 5 nm goat anti-mouse plus 10 nm goat anti-rabbit or 10 nm goat anti-mouse plus 5 nm goat anti-rabbit, respectively. For double labeling using antibodies made in the same species, the first primary antibody and the corresponding immunogold-conjugated antibody (5 nm gold) were applied, sections were exposed to paraformaldehyde vapor at 80°C for 1 hr, and the second primary antibody and its corresponding 10 nm gold antibody were applied the following day (Wang and Larsson, 1985; Matsubara et al., 1996; Zhao et al., 1998). Primary antibody combinations using this method included SAP-102 (JH62514) followed by NR2A/B or PSD-93 (AL) followed by SAP-102 (JH62514). Controls included the absence of the primary antibodies and incubation in 10 nm goat anti-rabbit or 10 nm goat anti-mouse or 5 nm goat anti-rabbit plus 15 nm goat anti-mouse immunogold, each for P2, P10, and P35. Gold labeling was very rare in control sections.

Immunogold particles were counted in the postsynaptic density and cleft, as in previous studies (Wang et al., 1998; Zhao et al., 1998; Petralia et al., 1998, 1999). All synapses were counted in a selected portion of the CA1 stratum radiatum of the hippocampus, as in a previous study (Petralia et al., 1999). Synapses were evaluated for the number of gold particles per synapse (both labeled and unlabeled) or number of gold particles per labeled synapse; labeled synapses had one or more gold particles. The number of gold particles per unit length of the synapse was not calculated because the results of such measurements done in conjunction with the previous study were generally similar to the number of gold particles per synapse (R. S. Petralia, J. A. Esteban Y.-X. Wang, J. G. Partridge, H.-M. Zhao, R. J. Wenthold, and R. Malinow, unpublished data). A lack of significant developmental change in synapse length seems to be typical of synapses of the CNS (Vaughn, 1989; Zhao et al., 1998). All micrographs used in the figures were processed with Adobe (Mountain View, CA) Photoshop 4.0 to optimize brightness and contrast.

Synapses used in this study showed characteristic features of asymmetric synapses: postsynaptic density, cleft, and presynaptic vesicles. As noted by Petralia et al. (1999), synapses increase in number with age. Also, immature-looking synapses are more common at early ages. Fiala et al. (1998), using serial sections and three-dimensional analysis, suggest that there are four stages in the development of postsynaptic structures of most excitatory spine synapses in the CA1 region: filopodia, dendrite shaft synapse, stubby protrusion, and mature spine. In our study, we divided postsynaptic structures into three groups: dendrite shafts, protuberances, and spines. Protuberances are wider than long and may include both the stubby protrusions and the enlarged bases of filopodia described by Fiala et al. (1998). Our "spine" category may include some examples of enlarged apices of filopodia (especially at the early postnatal ages), which would not be identifiable in our material without serial reconstruction. Consistent with Fiala et al. (1998), synapses at P2 were mostly on dendrite shafts. In contrast, in adults, most synapses were on spines, and dendrite shaft synapses were rare.

RESULTS

Antibody characterization

Several commercially available and donated antibodies were tested by immunoblotting of transfected cell membranes and hippocampus homogenates to determine specificity (Fig. 1). Some of the antibodies recognized more than one member of the MAGUK family of proteins reflecting the sequence similarities among these proteins. Although such antibodies may be appropriate for Western blotting because of the different molecular weights of the proteins, they are not acceptable for immunocytochemistry to identify a single protein. Furthermore, some antibodies could not be used because they failed to interact with their antigens after processing for postembedding staining. For immunogold immunocytochemistry, based on specificity and reactivity, the following were used: both antibodies to SAP-102, PSD-95 (TL and JH62092), and PSD-93 (AL). In Western blots of hippocampus, these antibodies detected a single band that co-migrated with the appropriate protein in the transfected cell samples. To allow direct comparisons, the same antibodies were used for Western blotting. For immunoprecipitation, SAP-97 (JH62426), PSD-93 (AL), either the PSD-95 (T60) or the PSD-95 (clone 7E3–1B8), and SAP-102 (JH62514) were effective. The PSD-95 (T60) has a slight cross-reaction with SAP-97, but the low expression of SAP-97 in the hippocampus allows us to use this antibody as one specific for PSD-95. The PSD-95 (clone 7E3-1B8) antibody has a slight cross-reaction with PSD-93 but does not cross-react with SAP-102. The PSD-95 antibody from TL is less effective for immunoprecipitation.

Western blot analysis of rat hippocampus shows different patterns for PSD-93/PSD-95 versus SAP-102 during development

As an initial step, we determined the patterns of expression of AMPA and NMDA receptor subunits and MAGUKs during postnatal development in the hippocampus (Figs. 2, 3). AMPA receptor subunits and the NR1 subunit showed similar patterns of development with a general increase with time after birth. Individually, NR2A and NR2B showed opposite patterns: NR2A immunoreactivity was undetectable at P2 and began to be elevated from P10 to 6 months, whereas NR2B was strongly expressed at P2 and showed a substantial decrease by 6 months. However, the combination of NR2A and NR2B, determined with an antibody that recognized both subunits, showed a pattern similar to that of NR1 and the AMPA receptor subunits. Analysis of the MAGUKs showed that SAP-102 was already highly expressed at P2. The SAP-102 expression increased during the first week and remained similar through P35 with a reduction in expression at 6 months. The temporal patterns of expression of both PSD-93 and PSD-95 are similar. PSD-93 and PSD-95 were expressed at low levels with detection beginning at P10 and

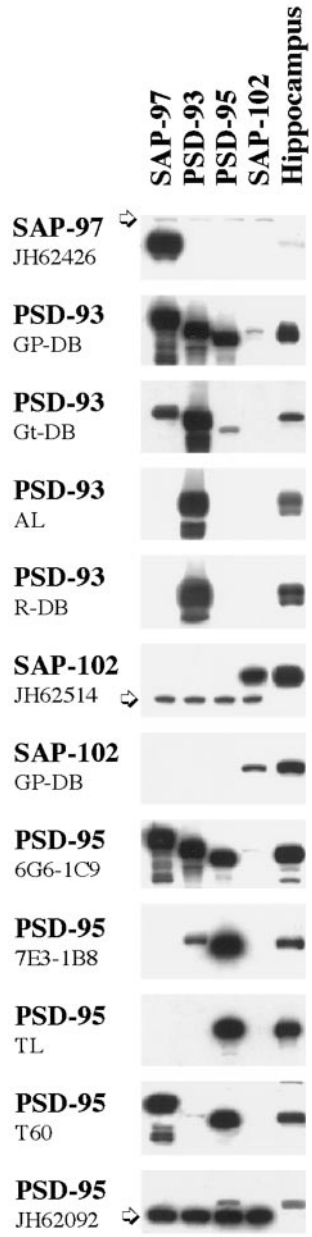

Figure 1. Specificity of antisera to MAGUKs. Western blot analysis reveals that the SAP-97 antiserum does not cross-react with the other PDZ proteins and gives a band corresponding to ~120 kDa in HEK293 transfected cells. As shown previously (Müller et al., 1995), SAP-97 is not heavily expressed in hippocampus. The anti-rabbit PSD-93 polyclonal antibodies (AL and R-DB) show the same specificity for PSD-93 in transfected cells and in adult hippocampus. In rat hippocampus, at least two bands at ~103–110 kDa can be detected. By similar analysis, the SAP-102 (JH62514 or GP-DB) antibodies recognize their antigens but show no cross-reactivity with the other members of the MAGUK family. PSD-95 (TL and JH62092) antibodies are the most specific antibodies against PSD-95 available. T60 anti-PSD-95 is a polyclonal antibody that reacts with PSD-95 as strong as with SAP-97 in transfected cells. In hippocampus, in addition to the 95 kDa specific band, we find two additional lighter bands at ~170 and 85 kDa. The *arrows* indicate a nonspecific band which appears only in transfected cells. *AL*, Alomone Laboratories; *GP*, guinea pig; *Gt*, goat; *R*, rabbit; *TL*, Transduction Laboratories.

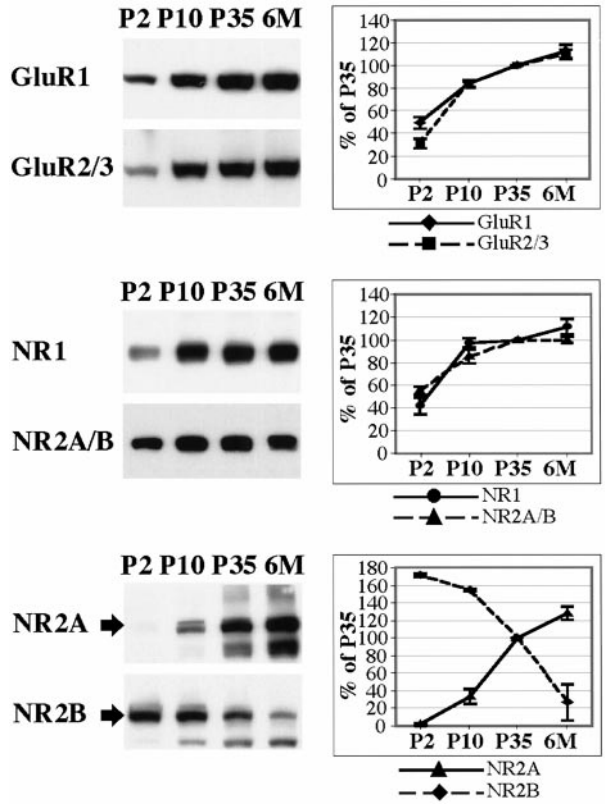

Figure 2. Patterns of developmental expression of the glutamate receptor subunits GluR1, GluR2/3, NR1, NR2A/B, NR2A, and NR2B. P2, P10, P35, and 6 month (*6M*) rat hippocampus homogenates (20 μg of protein/lane) were analyzed by SDS-PAGE and immunoblotting with affinity-purified antibodies: GluR1 (9T), GluR2/3 (25-8), NR1 (clone 54.1), NR2A/B (T12), NR2A (T58), and NR2B (T51). At all ages, samples analyzed with the different antibodies were obtained from the same preparation of hippocampus. Histograms show the relative amount of protein (in percent P35). Levels were measured by densitometric scanning of Western blots.

increasing throughout development. SAP-97 expression in the hippocampus was detected but at a level lower than that seen in other brain areas such as cortex and cerebellum (data not shown). Western blots labeled for PSD-93 and SAP-102 showed several bands, probably reflecting the presence of splice variants, which have been reported for both proteins (Brenman et al., 1996a,b; Müller et al., 1996). Other antibodies to the same proteins showed comparable patterns of expression during development (data not shown).

Development of PSD-95/SAP-102 proteins at the synapse

Immunogold labeling for PSD-95 (TL) and for SAP-102 (JH62514) in the CA1 region of the hippocampus was concentrated along the postsynaptic membrane and in the postsynaptic density (Fig. 4). For PSD-95, labeling in synapses increased approximately threefold from P2 to adult (P35) but showed little or no increase from P35 to 6 months (Table 2, Fig. 4*C*). The percent labeled synapses doubled from P2 to adult, whereas there was only a small increase in the number of gold particles in a labeled synapse during this time; the latter increase was not significant for any age. This indicates that the increase in PSD-95 during development is attributable primarily to an increase in the number of synapses containing PSD-95.

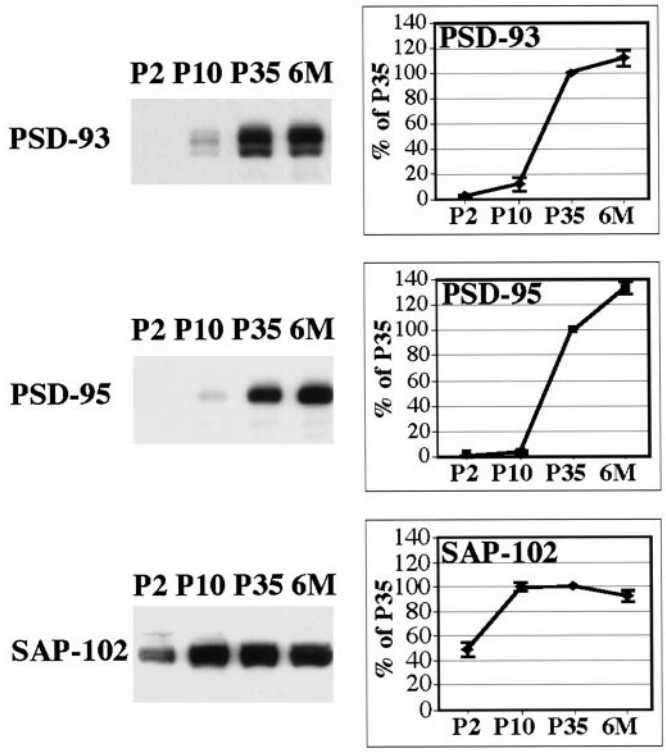

Figure 3. Patterns of developmental expression of MAGUKs. P2, P10, P35, and 6 month (*6M*) rat hippocampus homogenates (20 μg of protein/lane) were analyzed by SDS-PAGE and immunoblotting with antibodies against PSD-93 (AL), SAP-102 (JH62514), and PSD-95 (TL). At all ages, samples analyzed with the different antibodies were obtained from the same preparation of hippocampus. Histograms show the relative amount of protein (in percent P35). Levels were measured by densitometric scanning of Western blots.

In contrast to PSD-95, labeling for SAP-102 in synapses decreased by approximately half from P2 to adult and decreased further by 6 months (Table 2, Fig. 4*C*). Both the percent labeled synapses and the number of gold particles in a labeled synapse decreased during development, unlike the pattern seen for PSD-95. This indicates that the decrease in SAP-102 during development depends on a decrease in the number of synapses containing SAP-102 and on the density of SAP-102 labeling in a synapse.

To determine whether PSD-95 and SAP-102 are present in the same synapse, double labeling was done. Percent double labeling for SAP-102 and PSD-95 was highest at P35 (31%), when both the density at synapses and percent labeled synapses have similar values for the two proteins (Fig. 5). Lower levels of double labeling were found at P2 (13%), P10 (16%), and 6 months (17%), all times when the number of gold particles per synapse is very different between the two proteins. Overall, the developmental changes in percent double-labeling appear to reflect only a random distribution; we find no evidence for synapse populations that contain only SAP-102 or only PSD-95.

A number of other antibodies were used to confirm the above findings. Other antibodies to PSD-95 (JH62092; Fig. 4*A*) and SAP-102 (GP-DB; Fig. 4*B*) showed similar patterns of increasing and decreasing labeling, respectively, during development. Thus for PSD-95 (JH62092), percent labeled synapses increased with age: P2, 16%; P10, 29%; P35, 42%; for SAP-102 (GP-DB), percent labeled synapses decreased with age: P2, 76%; P10, 61%; P35, 33%. An antibody to PSD-93 (AL) showed a pattern of increasing labeling of synapses from P2 to adult that was very similar to the pattern obtained with the two PSD-95 antibodies (Fig. 6). In contrast, another PSD-93 antibody (GP-DB), which recognizes PSD-93, as well as PSD-95, SAP-97, and SAP-102, showed an increase in labeling from P2 to P10 but little change from P10 to adult, probably reflecting simultaneous changes in several proteins (data not shown).

Finally, to determine whether PSD-93 is present in the same synapses as PSD-95 or SAP-102, double-labeling was done in adults. Sixteen percent of synapses ($n = 116$) were double-labeled for PSD-93 (AL) and SAP-102 (JH62514), whereas 33% ($n = 106$) were double-labeled for PSD-93 (AL) and PSD-95 (TL). Thus, PSD-93 co-localizes with both SAP-102 and PSD-95 in these synapses and may co-localize more commonly with PSD-95.

Comparison of labeling for PSD-95 and SAP-102 in different postsynaptic structures (shaft, protuberance, or spine) during development did not reveal any consistent pattern (data not shown). However, there was an indication that, at least for SAP-102 at P2, SAP-102 is lower (gold/synapse) in dendrite shaft synapses than in spine synapses. This would be consistent with a model in which most dendrite shaft synapses at P2 develop into spine synapses (Fiala et al., 1998), and SAP-102 levels increase in the initial stages of synapse development.

Relationship between NMDA receptor subunits and PSD-95 and SAP-102

The developmental patterns of PSD-95 and SAP-102, both from Western blots of hippocampus and immunogold analysis of CA1 synapses, suggest a possible relationship between these proteins and the NR2 subunits NR2A and NR2B. In particular, the high expression of NR2B at young ages coincides with the earlier expression of SAP-102, whereas the later expression of NR2A coincides with that of PSD-93 and PSD-95. This raises the possibility that SAP-102 is primarily associated with NR2B and that PSD-93 and PSD-95 are primarily associated with NR2A. To test this hypothesis, we did co-immunoprecipitation analyses on NR2A, NR2B, SAP-97, PSD-93, PSD-95, and SAP-102. DOC-solubilized membranes from whole hippocampus or from the CA1–CA2 region of P2 and P35 rats were immunoprecipitated with anti-NR2A, anti-NR2B, anti-PSD-97, anti-PSD-93, anti-PSD-95, and anti-SAP-102 antibodies and analyzed by Western blotting using antibodies to NMDA receptor subunits (NR1, NR2A, and NR2B), PSD-97, PSD-93, PSD-95, and SAP-102 and AMPA receptor subunits (as controls). Co-immunoprecipitation of NR2A and NR2B occurred to some extent in both whole hippocampus (Fig. 7*A*) and CA1–CA2 (Fig. 7*B*), consistent with several reports showing that NMDA receptor complexes that contain NR2A, NR2B, and NR2A/NR2B co-exist in individual neurons (Blahos and Wenthold, 1996; Kew et al., 1998). Antibodies to NR2A or NR2B co-immunoprecipitated both PSD-95 and SAP-102 with an apparent preference for NR2A/PSD-95 and NR2B/SAP-102 (Fig. 7). Moreover, PSD-93, PSD-95, and SAP-102 co-immunoprecipitated both NR2A and NR2B with a preference for NR2A/PSD-93/95 and NR2B/SAP-102 (Fig. 8). The interaction cannot be quantified directly, because different antibodies, which are likely to have different affinities, were used. However, an indication of the interactions can be obtained by comparing the relative amounts of co-immunoprecipitating protein. Using this approach, we find that 3.8 ± 0.3% of PSD-95 and 3.7 ± 0.5% of SAP-102 co-immunoprecipitated with NR2A, whereas 2.3 ± 0.4% of PSD-95 and 6.2 ± 0.5% of SAP-102 co-immunoprecipitated with NR2B (for PSD-95, $n = 7$; for SAP-

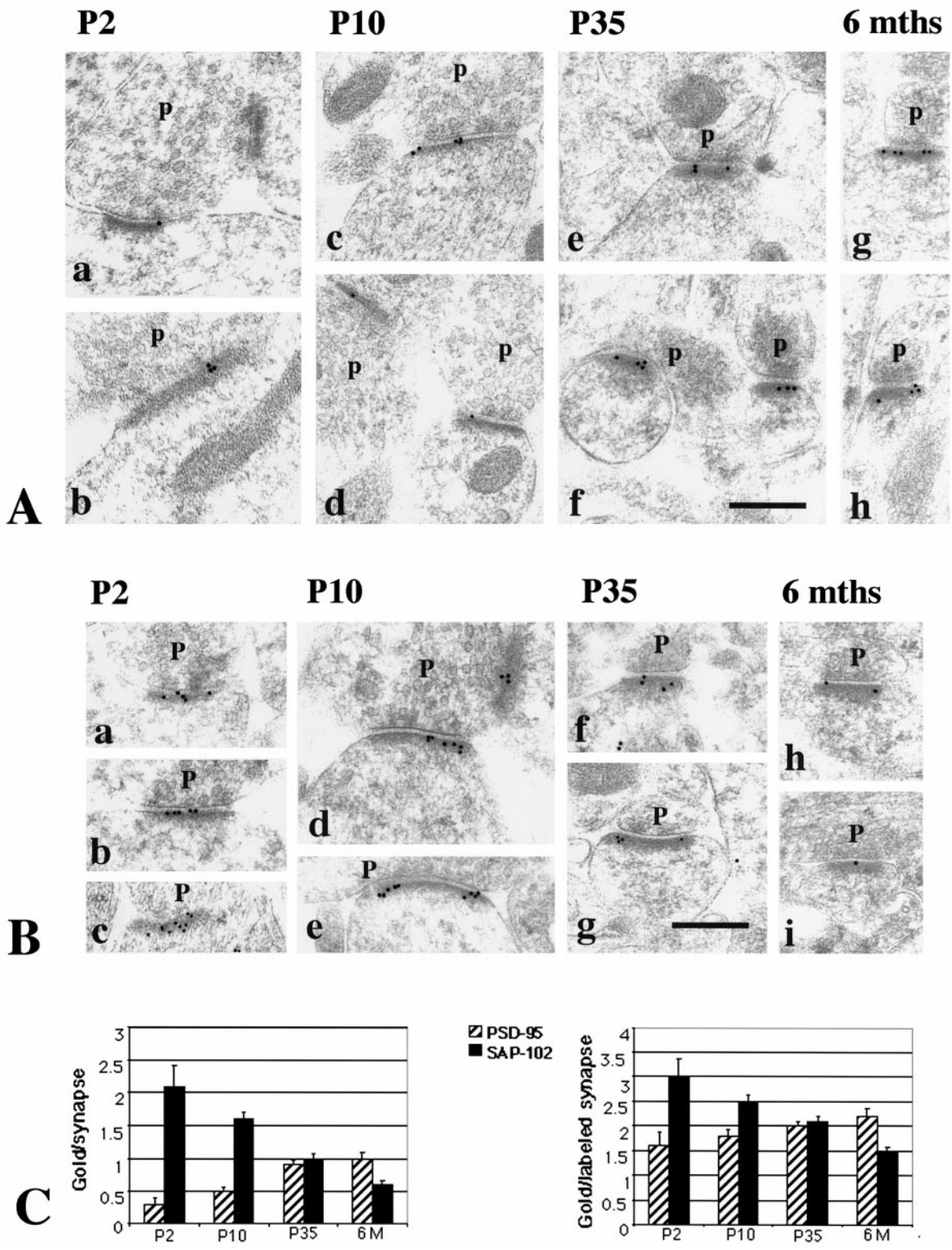

Figure 4. *A,* Immunogold labeling of PSD-95 in the CA1 stratum radiatum of the hippocampus. Postembedding immunogold labeling (10 nm) was performed using either of two PSD-95 antibodies (*b–e, g, h*, M, TL; *a, f*, R, JH), at P2 (*a, b*), P10 (*c, d*), P35 (*e, f*), and 6 months (*g, h*). *p*, Presynaptic terminal. Postsynaptic structures include dendrite shafts (*b,* synapse in *a*, *top right*) and spines (*c–h*); the synapse in the *bottom left* of *a* is at the enlarged base of a filopodium extending to the left (data not shown). Scale bar, 0.3 μm. Representative micrographs were chosen to illustrate the increase in PSD-95 labeling in synapses with age. *B,* Immunogold labeling of SAP-102 in the CA1 stratum radiatum of the hippocampus. Postembedding immunogold labeling (10 nm) was done using either of two SAP-102 antibodies (*a, b, d–f, h, i*, R, JH; *c, g*, GP-DB) at P2 (*a–c*), P10 (*d, e*), P35 (*f, g*), and 6 months (*h, i*). *p*, Presynaptic terminal. Postsynaptic structures include dendrite shafts (*b*), protuberances (*a, c*), and spines (*d–i*). Scale bar, 0.3 μm. Representative micrographs were chosen to illustrate the decrease in SAP-102 labeling in synapses with age. *C,* Summary of developmental changes in the number of gold particles per synapse and the number of gold particles per labeled synapse (see Table 2) at P2, P10, P35, and 6 months (*6M*). Error bars indicate SE.

Table 2. Summary of immunogold labeling for PSD-95 and SAP-102

	P2	P10	P35	6 months
PSD-95				
Particles/synapse	0.29 ± 0.09*	0.51 ± 0.06**	0.94 ± 0.06	0.97 ± 0.10
Percent synapses labeled	18	29	48	45
Particles/labeled synapse	1.58 ± 0.26	1.78 ± 0.13	1.96 ± 0.08	2.15 ± 0.16
No. of synapses	66	258	421	204
SAP-102				
Particles/synapse	2.12 ± 0.31	1.57 ± 0.11**	1.04 ± 0.07**	0.63 ± 0.06
Percent synapses labeled	71	63	49	43
Particles/labeled synapse	3.00 ± 0.36	2.48 ± 0.13*	2.11 ± 0.10**	1.48 ± 0.08
No. of synapses	65	245	373	191

The average number of gold particles per synapse was significantly different (*t* test, two-sample assuming unequal variances, two-tailed; $p < 0.01$) for PSD-95 (TL) and SAP-102 (JH62514) between P2 and P35, P2 and 6 months, P10 and P35, and P10 and 6 months. Significant differences also were seen for PSD-95 between P2 and P10 ($p < 0.05$) and for SAP-102 between P35 and 6 months ($p < 0.01$). For the average number of gold particles per labeled synapse, no significant difference was seen for any combination of ages for PSD-95 ($p < 0.01$), whereas significant differences were seen for SAP-102 between P2 and P35, P10 and P35 ($p < 0.05$), P2 and 6 months, P10 and 6 months, and P35 and 6 months ($p < 0.01$).

*Difference between two ages (left and right of symbol) significant at $p < 0.05$.

**Difference between two ages significant at $p < 0.01$.

102, $n = 7$). Immunoprecipitation with antibodies to PSD-95 and SAP-102 showed similar results: 2.9 ± 0.3% of NR2A and 1.9 ± 0.4% of NR2B co-immunoprecipitated with PSD-95, whereas 1.6 ± 0.3% of NR2A and 3.3 ± 0.5% of NR2B co-immunoprecipitated with SAP-102 (for NR2A, $n = 9$; for NR2B, $n = 6$). Thus, these analyses support a slight but not complete preference for NR2A/PSD-95 and NR2B/SAP-102 association. PSD-93 tends to behave as PSD-95 and interacts mostly with NR2A. At P2, when few NR2A complexes were found and PSD-93 or PSD-95 was poorly expressed, only NR2B co-immunoprecipitated with SAP-102 and vice versa (Fig. 9). SAP-97 was not abundant in the hippocampus, but some GluR2/3/SAP-97 complexes were found (Fig. 8). Moreover, SAP-97 did not seem to associate with NMDA receptors in the hippocampus, although an interaction between SAP-97 and NR2A has been shown in yeast experiments (Bassand et al., 1999).

A qualitative examination of double labeling for SAP-102 and NR2A/B or PSD-95 and NR2A/B at P2, P10, and P35 showed some double labeling at all ages, although no particular pattern was evident (data not shown). This is not surprising because the NR2A/B antibody recognizes both subunits and cannot distinguish between individual patterns of NR2A or NR2B. Specific antibodies for NR2A and NR2B were not used for immunocytochemistry, because they recognize additional proteins. In addition to distinctive synaptic associations, single-label studies with antibodies to PSD-95, SAP-102, and NMDA receptors and double labeling for SAP-102 and NR2A/B showed that all of these proteins are present in nonsynaptic surface specializations (Fiala et al., 1998). These structures resemble postsynaptic densities; they are adjacent to various nonsynaptic structures or to an empty fluid-filled space (a common feature in the neuropil at early postnatal ages). Nonsynaptic surface specializations were most common at P2, when they labeled commonly with antibodies to NR1, NR2A/B, and SAP-102 and less commonly with antibody to PSD-95 (Fig. 10).

SAP-102, PSD-95, and AMPA receptors

We have previously demonstrated that the synaptic expression of AMPA receptors in hippocampal synapses occurs later in development than does that of NMDA receptors (Petralia et al., 1999), raising the possibility that PSD-95 synaptic expression is related to the acquisition of AMPA receptors at these synapses. To test this, double-labeling analysis was done with antibodies to the AMPA receptor subunits GluR2/3 and PSD-95. Analysis was done at P10 when expression of both proteins is relatively low in synapses (29% of synapses were labeled for PSD-95, and 38% were labeled for GluR2/3; Petralia et al., 1999). However, only 10% of the synapses were double-labeled (data not shown), suggesting that there is no apparent relationship between the expression of GluR2/3 and PSD-95 in synapses during development.

DISCUSSION

In the present study, we investigated the synaptic association of SAP-97, PSD-93, SAP-102, and PSD-95 during postnatal development in the rat hippocampus. Our major findings show that (1) SAP-102 is present at high levels at most synapses at P2 and decreases through 6 months of age, whereas PSD-95 and PSD-93 are low at P2 and increase through 6 months; (2) Increases in synaptic PSD-95 are attributable primarily to an increase in the number of synapses containing PSD-95, whereas decreases in SAP-102 result from a decrease in both the number of synapses containing SAP-102 and the density of SAP-102 labeling in the synapse; (3) immunogold co-localization shows that multiple MAGUKs are expressed at the same synapse, indicating that PSD-93 and PSD-95 may be added to synapses that already contain SAP-102; (4) the developmental increase in synaptic PSD-93/95 correlates with increases in NR2A; immunoprecipitation does not show a strict relationship between NR2A and PSD-93/95 or NR2B and SAP-102 but indicates a preference for this pattern of interaction; and (5) the developmental increase in PSD-95 also correlates with the increase in synaptic AMPA receptors, but co-localization analysis does not show a relationship between PSD-95 and AMPA receptors at individual synapses.

Our results show that SAP-102 is highly expressed at CA1–CA2 synapses in young rats and tends to decline with development. In contrast, PSD-93 and PSD-95 appear to be expressed later, when AMPA receptors are common at these synapses. These patterns fit those previously reported for whole brain, as determined with Western blotting or *in situ* hybridization (Cho et

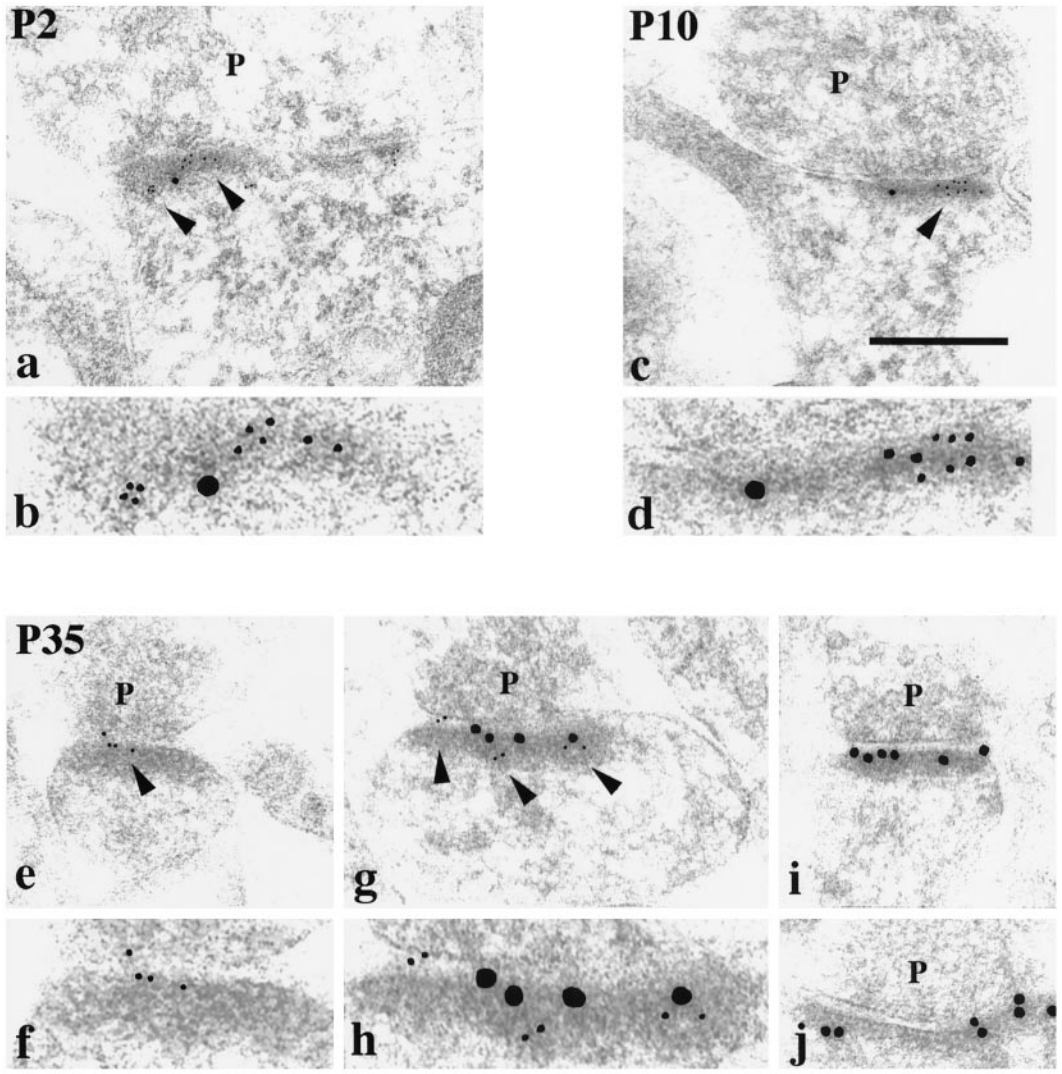

Figure 5. Double labeling for SAP-102 (R, JH; 5 nm gold) and PSD-95 (M, TL; 15 nm gold) in the CA1 stratum radiatum of the hippocampus, at P2 (*a, b*), P10 (*c, d*), and P35 (*e–j*). Five nanometer gold in *a, c, e*, and *g* is indicated by *arrowheads* and shown at a higher magnification in *b, d, f*, and *h*, respectively. *p*, Presynaptic terminal. Postsynaptic structures include dendrite shafts (*a, b*), protuberances (*c, d*), and spines (*e–j*). Scale bar: *a, c*, 0.3 μm; *e, g, i, j*, 0.2 μm; *b, d, f, h*, 0.1 μm. Representative micrographs were chosen to illustrate the decrease in SAP-102 and the increase in PSD-95 in synapses with age, and to show examples of single- and double-labeled synapses in adults.

al., 1992; Müller et al., 1996; Song et al., 1999; Wyszynski et al., 1999), suggesting that the developmental pattern we find at hippocampal synapses may be common to all CNS synapses. The dramatic enrichment of SAP-102 at young synapses, when other members of the MAGUK family are faintly expressed, may indicate an important role for SAP-102 in synaptogenesis. On the other hand, the expression of PSD-93 and PSD-95 later in development shows that these two proteins are not required for the early expression of NMDA receptors at synapses and suggests a role for these proteins in the mature and less plastic synapse. The number of synapses that are immunolabeled with PSD-95 antibodies increases sharply during development, but the number of gold particles per labeled synapse, reflecting the number of PSD-95 molecules present at the synapse, does not significantly change from P2 through 6 months of age. Such a pattern of expression suggests that the acquisition of PSD-95 may be regulated at the level of the individual synapse, rather than reflecting the total cellular expression levels as indicated by Western blots. The decrease in synaptic SAP-102 with age is gradual, suggesting

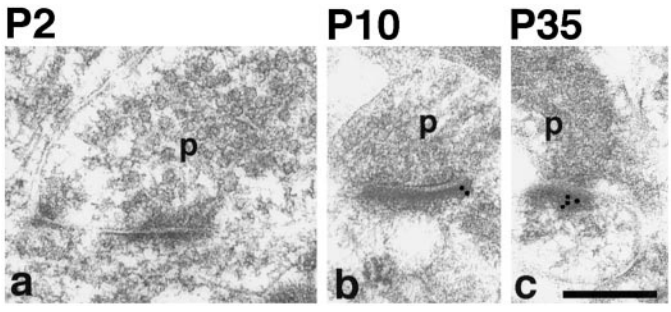

Figure 6. Immunogold labeling of PSD-93 (R, AL) in the CA1 stratum radiatum of the hippocampus. Postembedding immunogold labeling (10 nm) was performed at P2 (*a*), P10 (*b*), and P35 (*c*). *p*, Presynaptic terminal. Postsynaptic structures include dendrite shafts (*a, b*) and spines (*c*). Scale bar, 0.3 μm. Representative micrographs were chosen to illustrate the increase in PSD-93 labeling in synapses with age, similar to that seen for PSD-95.

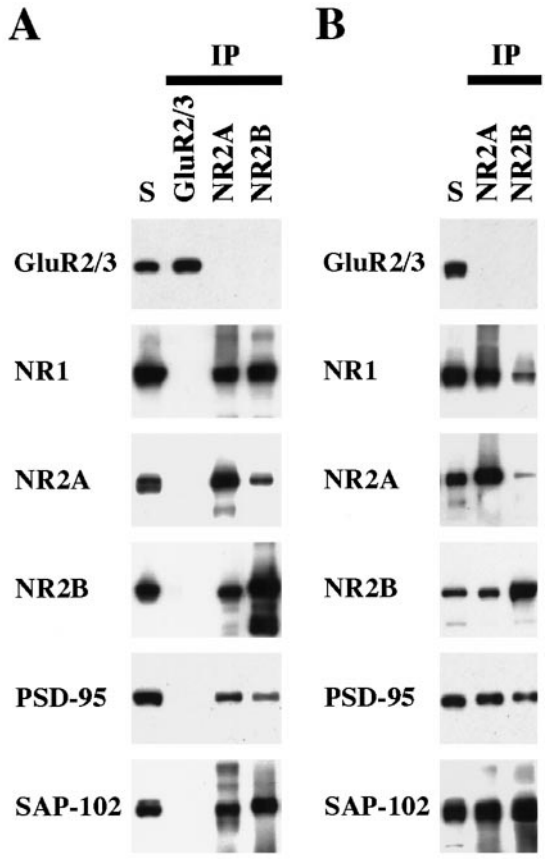

Figure 7. Co-immunoprecipitation of PSD-95 and SAP-102 with NR2 subunits. Whole hippocampus (*A*) or the CA1–CA2 region of the hippocampus (*B*) was solubilized in 1% DOC, and GluR2/3, NR2A, or NR2B were immunoprecipitated using 25-8 (GluR2/3) antibody, T58 NR2A serum, or T51 NR2B serum. Ten microliters of the total soluble protein (*S*) and 10 μl of the bound immunoprecipitate fractions were resolved by SDS-PAGE and probed with GluR2/3 (25-8), NR1 (clone 54.1), NR2A (2F6.3D5), NR2B (TL), PSD-95 (TL), and SAP-102 (JH62514). Because the immunoprecipitates were resuspended in 0.1 volume of the original soluble fraction, the bound sample is 10 times more concentrated than the total soluble fraction.

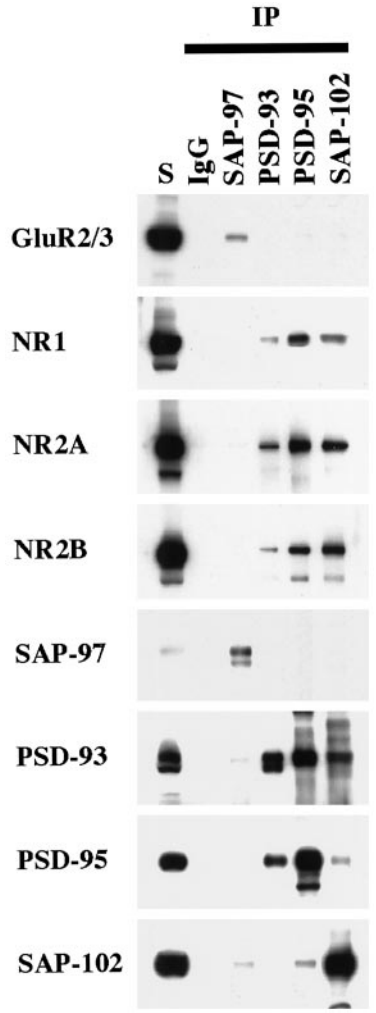

Figure 8. Co-immunoprecipitation of NR subunits with PSD-93, PSD-95, or SAP-102 in whole hippocampus. Hippocampi were solubilized in 1% DOC, and SAP-97, PSD-93, PSD-95, and SAP-102 were immunoprecipitated using JH62426, PSD-93 AL, T60, or JH62514 sera, respectively. Ten microliters of the total soluble protein input (*S*) and 10 μl of the bound immunoprecipitate fractions were separated by SDS-PAGE, immunoblotted, and incubated with antibodies against GluR2/3 (25-8), NR1 (clone 54.1), NR2A (2F6.3D5), NR2B (TL), SAP-97 (JH62426), PSD-93 (R-DB), PSD-95 (TL), or SAP-102 (JH62514). Because the immunoprecipitates were resuspended in 0.1 volume of the original soluble fraction, the bound sample is 10 times more concentrated than the total soluble fraction.

that the synaptic expression may be related to the general cellular levels of SAP-102, like that seen on Western blots. These different patterns of acquisition and loss also suggest that the switch from SAP-102 to PSD-95 is not a simple replacement of NMDA receptor anchors.

Our results highlight several differences between expression determined by Western blotting and expression determined by immunocytochemistry of the synapse. For example, the Western blot analysis shows a significant increase in SAP-102 protein during the first week after birth and a decrease between P35 and 6 months. However, the percent of synapses labeled and the particles per labeled synapse decrease gradually with age, with P2 showing the highest labeling. These discrepancies could arise in two ways. First, our Western blots are of the entire hippocampus, whereas our immunocytochemistry is restricted to synapses on CA1–CA2 pyramidal cell dendrites. Expression patterns may vary in different areas and cell types of the hippocampus. Second, total cellular expression and synaptic expression may not match. We tend to favor this explanation, because SAP-102 is abundant in cytoplasm (Müller et al., 1996; our unpublished data). Furthermore, the AMPA receptor subunit GluR1 can show developmental changes in intracellular levels that do not match changes in synaptic levels (Shi et al., 1999).

We investigated several mechanisms that may be involved in the regulation of the acquisition of PSD-93 and PSD-95. One explanation for our results is that PSD-95 and SAP-102 are present at different populations of synapses, and that the population containing PSD-95 develops later than the one containing SAP-102. This seems unlikely, because at P2 most synapses (71%) contain SAP-102. Double-label immunogold analyses show that, at all ages, some synapses express both PSD-95 and SAP-102, as well as PSD-93 and PSD-95, indicating that there is a mixture of MAGUKs at any one synapse. Therefore, these data suggest that the addition of PSD-95 occurs predominantly at synapses that already contain SAP-102. An alternative explanation is that early SAP102-containing synapses are lost, and new

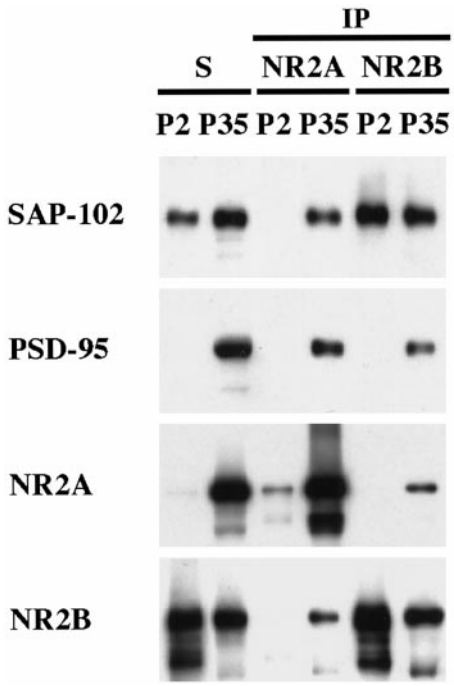

Figure 9. Comparison of co-immunoprecipitation of PSD-95 and SAP-102 with NR2 subunits at P2 and P35. P2 and P35 hippocampi were solubilized in 1% DOC, and the same amount of protein was used for immunoprecipitation of NR2A and NR2B using T58 NR2A or T51 NR2B sera, respectively. Total soluble protein (*S*) and the bound immunoprecipitate fractions were resolved by SDS-PAGE and probed with NR2A (2F6.3D5), NR2B (TL), PSD-95 (TL), and SAP-102 (JH62514).

synapses, containing both SAP-102 and PSD-95, are formed. Our finding that PSD-93, PSD-95, and SAP-102 can be co-localized at the same synapse is consistent with studies demonstrating interactions between individual MAGUKs and indicates that these interactions occur at synapses and are likely to be functionally significant. PSD-95 forms homomultimers via its N-terminal domain (Hsueh et al., 1997) and heteromultimers with PSD-93 (Kim et al., 1996). Also, it was recently demonstrated that SAP-102 and PSD-95 can interact with each other in the presence of Ca^{2+} and calmodulin (Masuko et al., 1999).

Our data show a close correspondence between the developmental patterns of NR2B and postsynaptic SAP-102 and between the developmental patterns of NR2A and postsynaptic PSD-93/95. Such a pattern is expected if NR2B is associated with SAP-102 and NR2A is associated with PSD-93/95, as has been proposed in the retina (Koulen et al., 1998a,b). To address this possibility, we studied the co-immunoprecipitation properties of these proteins in the young and the adult hippocampus. In the P2 hippocampus, we find that NMDA complexes contain mainly NR2B associated with SAP-102. In adult hippocampus, we find that NMDA receptor complexes containing either NR2B alone or NR2A alone are predominant, although some complexes are found containing both NR2 subunits. These results are consistent with reports showing that single neurons can contain three types of NMDA receptors, those with only NR2A, only NR2B, and both NR2A and NR2B (Kew et al., 1998). In these immunoprecipitation studies, we did not see an absolute bias for an association of NR2A and PSD-93/95 or NR2B and SAP-102, although quantitation showed relatively more PSD-95 immunoprecipitating with NR2A and more SAP-102 immunoprecipitating with NR2B.

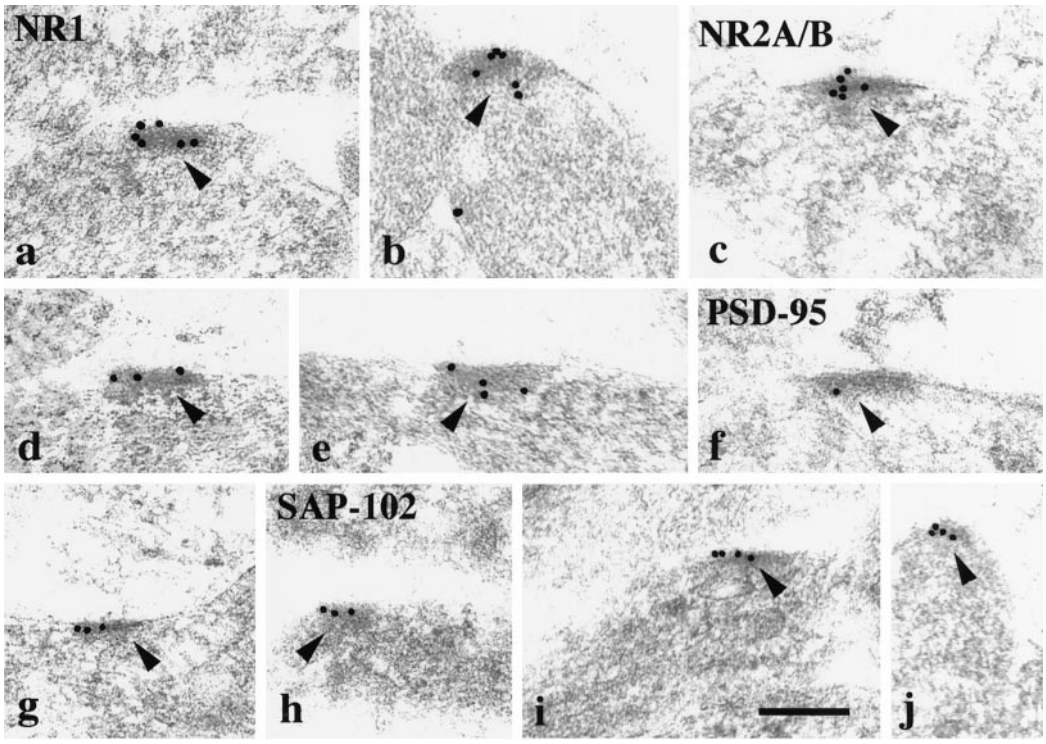

Figure 10. Immunogold labeling (10 nm gold) of NR1 (*a, b*), NR2A/B (*c–e*), PSD-95 (*f, g*; M, TL), and SAP-102 (*h–j*; R, JH) in nonsynaptic surface specializations (*arrowheads*) in the CA1 stratum radiatum of the hippocampus at P2. Scale bar, 0.2 μm.

Our results indicate that in hippocampus, SAP-102 is the earlier developmental anchor that may be involved in organizing NMDA receptors at synapses. These results differ from those reported for cultured hippocampal neurons by Rao et al. (1998), in which it was found that PSD-93, PSD-95, and guanylate kinase-associated protein were often present at synapse-like structures before NMDA receptors appeared. Thus, based on those results, it was suggested that PSD-93, PSD-95, and GKAP play a key role in synapse formation. More recently, Masuko et al. (1999) showed that SAP-102 and NR2B co-localize at synaptic sites in cultured rat hippocampal neurons. Although SAP-102 and PSD-95 were not simultaneously studied in cultures, the results of the culture studies (Rao et al., 1998) are inconsistent with ours, because we see NMDA receptors at synapses before PSD-95. A likely explanation is that formation of synapses in culture and *in vivo* are different, and that the mechanisms controlling critical events, such as the association of a receptor with a synaptic anchor, are not the same in culture as *in vivo*. Our results, however, would support the idea that SAP-102 is preceding the appearance of NMDA receptors at the synapse or at least that SAP-102 and NMDA receptors appear simultaneously at the synaptic sites. In searching for structures that may represent the early stages of a developing synapse, we have found nonsynaptic immunolabeling near the plasma membrane for NR1, NR2A/B, SAP-102, PSD-95, and double-labeled SAP-102 and NR2A/B, most commonly at P2. Synaptic Ras-GTPase-activity protein, which interacts with SAP-102 and PSD-95 (Kim et al., 1998), also was common in these structures (N. Sans, R. S. Petralia, Y.-X Wang, and R. J. Wenthold, unpublished data). Many of these have a dense appearance (Fiala et al., 1998), like a postsynaptic density, and it is not possible to determine whether they are new formations or remnants of former synapses.

Because PDZ domains 1 and 2 of SAP-102 and PSD-95 (and PSD-93) are similar, the functional consequences of changing these anchors may not be directly related to their association with NMDA receptors. Rather, it may reflect associations the anchors have with other molecules (for review, see Nagano et al., 1998; Kim and Huganir, 1999). For the most part, these interactions have not been demonstrated for all MAGUKs, but rather, it has been assumed that similar interactions occur based on their sequence similarities. From our results, it is important to know whether the same proteins interact with PSD-95 and SAP-102. PSD-95-mutant mice show a normal pattern of NMDA receptor expression (Migaud et al., 1998). Because our results show that synapses express both SAP-102 and PSD-95 (as well as PSD-93), receptors that are normally associated with PSD-95 would probably be linked with the remaining two anchors. The plasticity differences in the PSD-95-mutant mice, enhanced long-term potentiation and an absence of long-term depression, could arise from these abnormal associations. It will be interesting to determine whether the changes in synaptic expression of SAP-102 and PSD-95 during development are related to the physiological changes that occur during the critical period of development in the hippocampus and other structures.

REFERENCES

Bar-Peled M, Raikhel NV (1996) A method for isolation and purification of specific antibodies to a protein fused to the GST. Anal Biochem 241:140–142.

Bassand P, Bernard A, Rafiki A, Gayet D, Khrestchatisky M (1999) Differential interaction of the tSXV motifs of the NR1 and NR2A NMDA receptor subunits with PSD-95 and SAP-97. Eur J Neurosci 11:2031–2043.

Blahos IIJ, Wenthold RJ (1996) Relationship between NMDA receptor NR1 splice variants and NR2 subunits. J Biol Chem 271:15669–15674.

Brenman JE, Chao DS, Gee SH, McGee AW, Craven SE, Santillano DR, Wu Z, Huang F, Xia H, Peters MF, Froehner SC, Bredt DS (1996a) Interaction of nitric oxide synthase with the postsynaptic density protein PSD-95 and 1-syntrophin mediated by PDZ domains. Cell 84:757–767.

Brenman JE, Christopherson KS, Craven SE, McGee AW, Bredt DS (1996b) Cloning and characterization of postsynaptic density 93, a nitric oxide synthase interacting protein. J Neurosci 16:7407–7415.

Cho K-O, Hunt CA, Kennedy MB (1992) The rat brain postsynaptic density fraction contains a homolog of the *Drosophila* discs-large tumor suppressor protein. Neuron 9:929–942.

Christie JM, Wenthold RJ, Monaghan DT (1999) Insulin causes a transient tyrosine phosphorylation of NR2A and NR2B NMDA receptor subunits in rat hippocampus. J Neurochem 72:1523–1528.

Fiala JC, Feinberg M, Popov V, Harris KM (1998) Synaptogenesis via dendritic filopodia in developing hippocampal area CA1. J Neurosci 18:8900–8911.

Hartveit E, Brandstätter JH, Sassoè-Pognetto MS, Laurie DJ, Seeburg PH, Wässle H (1994) Localization and developmental expression of the NMDA receptor subunit NR2A in the mammalian retina. J Comp Neurol 348:570–582.

Hell JW, Westenbroek RE, Warner C, Ahlijanian MK, Prystay W, Gilbert MM, Snutch TP, Catterall WA (1993) Identification and differential subcellular localization of the neuronal class C and class D L-type calcium channel alpha 1 subunits. J Cell Biol 123:949–962.

Hsueh YP, Kim E, Sheng M (1997) Disulfide-linked head-to-head multimerization in the mechanism of ion channels clustering by PSD-95. Neuron 18:803–814.

Kennedy MB (1993) The postsynaptic density. Curr Opin Neurobiol 3:732–737.

Kennedy MB (1997) The postsynaptic density at glutamatergic synapses. Trends Neurosci 20:264–268.

Kew JN, Richards JG, Mutel V, Kemp JA (1998) Developmental changes in NMDA receptor glycine affinity and ifenprodil sensitivity reveal three distinct populations of NMDA receptors in individual rat cortical neurons. J Neurosci 18:1935–1943.

Kim E, Niethammer M, Rothschild A, Jan YN, Sheng M (1995) Clustering of Shaker-type K+ channels by interaction with a family of membrane-associated guanylate kinases. Nature 378:85–88.

Kim E, Cho K-O, Rothschild A, Sheng M (1996) Heteromultimerization and NMDA receptor-clustering activity of chapsyn-110, a member of the PSD-95 family of proteins. Neuron 17:103–113.

Kim JH, Huganir RL (1999) Organization and regulation of proteins at synapses. Curr Opin Cell Biol 11:248–254.

Kim JH, Liao D, Lau LF, Huganir RL (1998) SynGAP: a synaptic RasGAP that associates with the PSD-95/SAP90 protein family. Neuron 20:683–691.

Kistner U, Wenzel BM, Veh RW, Cases-Langhoff C, Garner AM, Appeltauer U, Voss B, Gundelfinger ED, Garner CC (1993) SAP90, a rat presynaptic protein related to the product of the *Drosophila* tumor suppressor gene dlg-A. J Biol Chem 268:4580–4583.

Kornau H, Seeburg P, Kennedy M (1997) Interaction of ion channels and receptors with PDZ domain proteins. Curr Opin Neurobiol 7:368–373.

Kornau HC, Schenker LT, Kennedy MB, Seeburg PH (1995) Domain interaction between NMDA receptor subunits and the postsynaptic density protein PSD-95. Science 269:1737–1740.

Koulen P, Garner CC, Wässle H (1998a) Immunocytochemical localization of the synapse-associated protein SAP 102 in the rat retina. J Comp Neurol 397:326–336.

Koulen P, Fletcher EL, Craven SE, Bredt DS, Wässle H (1998b) Immunocytochemical localization of the postsynaptic density protein PSD-95 in the mammalian retina. J Neurosci 18:10136–10149.

Lau LF, Mammen A, Ehlers MD, Kindler S, Chung WJ, Garner CC, Huganir RL (1996) Interaction of the *N*-methyl-D-aspartate receptor complex with a novel synapse-associated protein, SAP-102. J Biol Chem 271:21622–21628.

Leonard AS, Davare MA, Horne MC, Garner CC, Hell JW (1998) SAP97 is associated with the α-amino-3-hydroxy-5-methylisoxazole-4-propionic acid receptor GluR1 subunit. J Biol Chem 273:19518–19524.

Lue RA, Marfatia SM, Branton D, Chishti AH (1994) Cloning and characterization of hdlg: the human homologue of the *Drosophila* discs

large tumor suppressor binds to protein 4.1. Proc Natl Acad Sci USA 91:9818–9822.

Masuko N, Makino K, Kuwahara H, Fukunaga K, Sudo T, Araki N, Yamamoto H, Yamada Y, Miyamoto E, Saya H (1999) Interaction of NE-dlg/SAP102, a neuronal and endocrine tissue-specific membrane-associated guanylate kinase protein, with calmodulin and PSD-95/SAP90. A possible regulatory role in molecular clustering at synaptic sites. J Biol Chem 274:5782–5790.

Matsubara A, Laake JH, Davanger S, Usami S, Ottersen OP (1996) Organization of AMPA receptor subunits at a glutamate synapse: a quantitative immunogold analysis of hair cell synapses in the rat organ of Corti. J Neurosci 16:4457–4467.

Migaud M, Charlesworth P, Dempster M, Webster LC, Watabe AM, Makhinson M, He Y, Ramsay MF, Morris RGM, Morrison JH, O'Dell TJ, Grant SGN (1998) Enhanced long-term potentiation and impaired learning in mice with mutant postsynaptic density-95 protein. Nature 396:433–439.

Müller BM, Kistner U, Veh RW, Cases-Langhoff C, Becker B, Gundelfinger ED, Garner CC (1995) Molecular characterization and spatial distribution of SAP-97, a novel presynaptic protein homologous to SAP-90 and the *Drosophila* discs-large tumor suppressor protein. J Neurosci 15:2354–2366.

Müller BM, Kistner U, Kindler S, Chung WJ, Kuhlendahl S, Fenster SD, Lau LF, Veh RW, Huganir RL, Gundelfinger ED, Garner CC (1996) SAP102, a novel postsynaptic protein that interacts with NMDA receptor complexes *in vivo*. Neuron 17:255–265.

Nagano T, Jourdi H, Nawa H (1998) Emerging roles of Dlg-Like PDZ proteins in the organization of the NMDA-type glutamatergic synapse. J Biochem 124:869–875.

Niethammer M, Kim E, Sheng M (1996) Interaction between the C terminus of NMDA receptor subunits and multiple members of the PSD-95 family of membrane-associated guanylate kinases. J Neurosci 16:2157–2163.

Petralia RS, Yokotani N, Wenthold RJ (1994a) Light and electron microscope distribution of the NMDA receptor subunit NMDAR1 in the rat nervous system using a selective anti-peptide antibody. J Neurosci 14:667–696.

Petralia RS, Wang YX, Wenthold RJ (1994b) The NMDA receptor subunits NR2A and NR2B show histological and ultrastructural localization patterns similar to those of NR1. J Neurosci 14:6102–6120.

Petralia RS, Wang Y-X, Mayat E, Wenthold RJ (1997) Glutamate receptor subunit 2-selective antibody shows a differential distribution of calcium-impermeable AMPA receptors among populations of neurons. J Comp Neurol 385:456–476.

Petralia RS, Zhao H-M, Wang Y-X, Wenthold RJ (1998) Variations in the tangential distribution of postsynaptic glutamate receptors in Purkinje cell parallel and climbing fiber synapses during development. Neuropharmacology 37:1321–1334.

Petralia RS, Esteban JA, Wang Y-X, Partridge JG, Zhao H-M, Wenthold RJ, Malinow R (1999) Selective acquisition of AMPA receptors at hippocampus CA1 synapses during postnatal development. Nat Neurosci 2:31–36.

Rao A, Kim E, Sheng M, Craig AM (1998) Heterogeneity in the molecular composition of excitatory postsynaptic sites during development of hippocampal neurons in culture. J Neurosci 18:1217–1229.

Rubio ME, Wenthold RJ (1997) Glutamate receptors are selectively targeted to postsynaptic sites in neurons. Neuron 18:939–950.

Sheng M (1996) PDZs and receptor/channel clustering: rounding up the latest suspects. Neuron 17:575–578.

Sheng M, Kim E (1996) Ion channel associated proteins. Curr Opin Neurobiol 6:602–608.

Shi S-H, Hayashi Y, Petralia RS, Zaman SH, Wenthold RJ, Svoboda K, Malinow R (1999) Rapid spine delivery and redistribution of AMPA receptors after synaptic NMDA receptor activation. Science 284:1811–1816.

Song JY, Ichtchenko K, Sudhof TC, Brose N (1999) Neuroligin 1 is a postsynaptic cell-adhesion molecule of excitatory synapses. Proc Natl Acad Sci USA 96:1100–1105.

Vaughn JE (1989) Review: fine structure of synaptogenesis in the vertebrate central nervous system. Synapse 3:255–285.

Wang BL, Larsson LI (1985) Simultaneous demonstration of multiple antigens by indirect immunofluorescence or immunogold staining. Novel light and electron microscopical double and triple staining method employing primary antibodies from the same species. Histochemistry 83:47–56.

Wang YX, Wenthold RJ, Ottersen OP, Petralia RS (1998) Endbulb synapses in the anteroventral cochlear nucleus express a specific subset of AMPA-type glutamate receptor subunits. J Neurosci 18:1148–1160.

Wenthold RJ, Yokotani N, Doi K, Wada K (1992) Immunochemical characterization of the non-NMDA glutamate receptor using subunit-specific antibodies. Evidence for a hetero-oligomeric structure in rat brain. J Biol Chem 267:501–507.

Wyszynski M, Kim E, Yang FC, Sheng M (1999) Biochemical and immunocytochemical characterization of GRIP, a putative AMPA receptor anchoring protein, in rat brain. Neuropharmacology 37:1335–1344.

Zhao HM, Wenthold RJ, Petralia RS (1998) Glutamate receptor targeting to synaptic populations on Purkinje cells is developmentally regulated. J Neurosci 18:5517–5528.